REVIEW

MRI of the lung (3/3)—current applications and future perspectives

Jürgen Biederer · S. Mirsadraee · M. Beer · F. Molinari · C. Hintze · G. Bauman ·
M. Both · E. J. R. Van Beek · J. Wild · M. Puderbach

Abstract

Background MRI of the lung is recommended in a number of clinical indications. Having a non-radiation alternative is particularly attractive in children and young subjects, or pregnant women.

Methods Provided there is sufficient expertise, magnetic resonance imaging (MRI) may be considered as the preferential modality in specific clinical conditions such as cystic fibrosis and acute pulmonary embolism, since additional functional information on respiratory mechanics and regional lung perfusion is provided. In other cases, such as tumours and pneumonia in children, lung MRI may be considered an alternative or adjunct to other modalities with at least similar diagnostic value.

Results In interstitial lung disease, the clinical utility of MRI remains to be proven, but it could provide additional information that will be beneficial in research, or at some stage in clinical practice. Customised protocols for chest imaging combine fast breath-hold acquisitions from a "buffet" of sequences. Having introduced details of imaging protocols in previous articles, the aim of this manuscript is to discuss the advantages and limitations of lung MRI in current clinical practice.

Conclusion New developments and future perspectives such as motion-compensated imaging with self-navigated sequences or fast Fourier decomposition MRI for non-contrast enhanced ventilation- and perfusion-weighted imaging of the lung are discussed.

J. Biederer (✉) · C. Hintze · M. Both
Department of Diagnostic Radiology, University Hospital
Schleswig-Holstein, Campus Kiel,
Arnold-Heller-Straße. 3, Haus 23,
24105 Kiel, Germany
e-mail: juergen.biederer@rad.uni-kiel.de

S. Mirsadraee · E. J. R. Van Beek
Clinical Research Imaging Centre, University of Edinburgh,
47 Little France Crescent,
Edinburgh EH16 4TJ, UK

M. Beer
Department of Radiology, University Hospital Würzburg,
Josef-Schneider-Straße 2, Haus D31,
97080 Würzburg, Germany

F. Molinari
Department of Bioimaging and Radiological Sciences,
Catholic University of Rome, Gemelli Hospital,
L.go A. Gemelli 8,
00168 Rome, Italy

G. Bauman
Division of Medical Physics in Radiology,
German Cancer Research Center (DKFZ),
Im Neuenheimer Feld 280,
69120 Heidelberg, Germany

J. Wild
Academic Radiology, Royal Hallamshire Hospital Sheffield,
University of Sheffield,
Sheffield S10 2JF, UK

M. Puderbach
Department of Diagnostic and Interventional Radiology,
Chest Clinics at University Hospital Heidelberg,
Amalienstr. 5,
69126 Heidelberg, Germany

M. Puderbach
Department of Radiology,
German Cancer Research Center (DKFZ),
Im Neuenheimer Feld 280,
69120 Heidelberg, Germany

Main Messages

- *MRI evolves as a third lung imaging modality, combining morphological and functional information.*
- *It may be considered first choice in cystic fibrosis and pulmonary embolism of young and pregnant patients.*
- *In other cases (tumours, pneumonia in children), it is an alternative or adjunct to X-ray and CT.*
- *In interstitial lung disease, it serves for research, but the clinical value remains to be proven.*
- *New users are advised to make themselves familiar with the particular advantages and limitations.*

Keywords Magnetic resonance imaging · Cystic fibrosis · Pulmonary embolism · Tumor · Infiltrate · Functional imaging

Introduction

Magnetic resonance imaging (MRI) of the lung has been a challenge due to limitations such as low proton density in the lung and the fast signal decay due to susceptibility artefacts at air-tissue interfaces. Thanks to recent technical advances such as parallel imaging, shared echo-technique and rotating phase encoding, lung MRI can be recommended in a number of clinical indications [1].

The introduction into clinical routine is facilitated by customising comprehensive MR protocols that apply fast breath-hold acquisition techniques from a "buffet" of sequences that are optimised for chest imaging [2]. The basic imaging protocol comprises a non-contrast-enhanced protocol based on fast breath hold T1- and T2-weighted sequences to detect lung infiltrates, nodules or masses. Additional steady-state free precession sequence (SSFP) imaging can be performed with free breathing and is highly sensitive for detection of central pulmonary embolism, and provides information on respiratory mechanics [2, 3]. Respiration-triggered T2-weighted sequences are available for uncooperative patients and those with breath-holding difficulties [4]. The sensitivity of this basic protocol for infiltrates and lung nodules is reported to be similar to CT [5–7]. Additional contrast-enhanced fat-saturated three-dimensional gradient echo (3D-GRE) sequences are warranted for unclear masses, consolidations or pleural effusion detected in the basic protocol [8]. Three components are available for the assement of pulmonary vasculature and lung perfusion: An initial free-breathing unenhanced examination followed by dynamic contrast-enhanced perfusion imaging and a high-resolution angiogram [9].

With these customised protocols, lung MRI offers alternative solutions to routine diagnostic challenges, in particular for the imaging of the mediastinum. It also provides an alternative radiation-free diagnostic option that is especially relevant to young and pregnant patients, as well as subjects who need to undergo multiple investigations, e.g. for research purposes.

The details of the MR physics background as well as the protocol tree and its branches have been addressed in the two preceeding articles (citations 1/3 and 3/3). The aim of this paper is to discuss the advantages and limitations of lung MRI for a number of selected clinical applications and to outline current developments and future perspectives.

Clinical scenarios in which MRI might be considered a first choice modality

Cystic fibrosis

Cystic fibrosis (CF) lung disease is caused by mutations in the *CFTR* gene and remains one of the most frequent lethal inherited diseases in the Caucasian population. Due to the progress in therapy and management of CF lung disease in the past decades, the life expectancy of CF patients has increased substantially, with a current median survival of approximately 40 years and is expected to increase even further [10, 11]. It is known that clinical parameters including spirometric pulmonary function testing (PFT) suffer from limited sensitivity and provide no regional information. With the advances in imaging in general and the ability to characterise and quantify CF in greater detail, imaging will likely play an increasing role in the improved understanding of the disease process and the progression of disease. Furthermore imaging will serve as a biomarker for the development of new treatments.. However, this also means that it becomes vital to reduce the overall (cumulative) radiation burden in this population, as this could lead to iatrogenic carcinogenesis [12].

Magnetic resonance imaging (MRI) is reported to be comparable to CT with regard to the detection of morphological changes in the CF lung [13–15]. At the same time MRI is superior to CT when it comes to the assessment of functional changes such as altered pulmonary perfusion [16]. Moreover, using the described MR protocols, it is possible to visualise bronchiectasis, bronchial wall thickening, mucus plugging, air fluid levels, consolidation and segmental consolidation and destruction [13], (Fig. 1a, b).

The accuracy of MRI in detecting bronchiectasis is dependent on a number of factors, including bronchial level and diameter, wall thickness, and the signal from within the bronchial wall and lumen. Central bronchi and bronchiectasis (central, peripheral) are well visualised on MRI, whereas normal peripheral bronchi starting at the 3rd to 4th generation are poorly visualised. The depiction of bronchial wall

Fig. 1 A 29-year-old female with cystic fibrosis. The axial T2-weighted (BLADE; **a**) and the volumetric contrast-enhanced 3D-GRE (VIBE; **b**) breath-hold acquisitions show severe bronchiectasis, bronchial wall thickening, mucus plugging, pleural effusion as well as a destructed middle lobe. The perfusion subtraction image (**c**) shows a severely impaired perfusion pattern with loss of perfusion in several areas. The maximum enhancement (MAX) and time to peak anhancement (TTP maps) allow for a further characterisation of the perfusion impairment. Most areas with impaired perfusion show a reduced (MAX map) and delaid (TTP map) perfusion. Notice the area in the left upper lobe with reduced but not delayed perfusion (arrowhead)
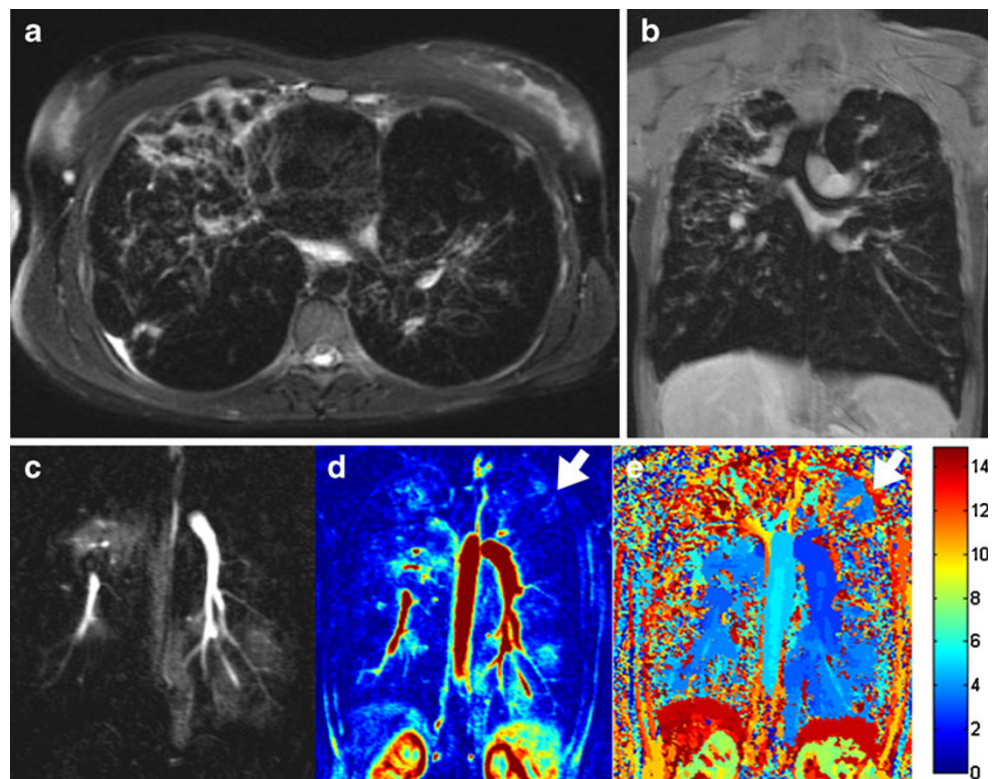
thickening depends on bronchial size and signal [13]. A high signal of the bronchial wall on T2-weighted (T2w) images represents increased fluid, i.e. oedema, possibly caused by active inflammation. Enhancement of the thickened bronchial wall on post-contrast, fat-suppressed T1-weighted images is thought to be related to inflammatory activity. It is important to note that compared to MRI, CT can only detect wall thickening and is not able to comment on the cause [13].

Mucus plugging is well visualised on MRI even down to the small airways due to the high T2 signal of its fluid content. It is recognised as a high T2 signal filling of the bronchus along its course with branching in the periphery giving a grape-like or tree-in-bud appearance, respectively. As mucus plugs do not enhance, they are easily differentiated from bronchial wall thickening [13].

Bronchial air fluid levels are indicative of active infection, occurring in saccular or varicose bronchiectasis, and can be visualised by their high T2 signal. However, discriminating a bronchus with an air fluid level from one with partial mucus plugging or a severely thickened wall can be difficult. When evaluating the signal characteristics on T2- and T1-weighted images with and without contrast enhancement, air fluid levels can usually be differentiated.

Pulmonary consolidation in CF is mainly caused by alveolar filling with inflammatory material leading to a high signal on T2w images. Comparable to CT, MRI is able to visualise air bronchograms as low signal areas following the course of the bronchi within the consolidation [17, 18]. With progression of the disease, complete destruction of lung segments or lobes can occur with similar appearances on MRI and CT.

Compared to CT, the strength of MRI is the additional assessment of "function", i.e. perfusion, pulmonary hemodynamics and ventilation. In CF, regional ventilatory defects cause changes in regional lung perfusion due to the hypoxic vasoconstriction response or tissue destruction. Using MRI, lung perfusion can be assessed by contrast-enhanced lung perfusion imaging [19]. Using contrast-enhanced 3D MRI, perfusion defects in 11 children with CF were reported to correlate well with the degree of tissue destruction [16]. Furthermore it was shown that at the age of 0–6 years lung perfusion changes were more prominent than morphological changes. However, establishing quantitative assessment tools for lung morphology is challenging for several reasons. First, signal intensities as derived from MRI are not calibrated as compared to CT. Second, the signal-to-noise ratio (SNR) in the lung is low and heterogeneous due to several physical circumstances [20]. Moreover, due to the lack of linearity between the MR signal and the concentration of applied contrast media, quantification of pulmonary perfusion using MRI is challenging [21]. Nevertheless, Risse et al. [22] described the importance of the qualitative assessment of the contrast time course component when analysing contrast-enhanced 3D MRI to categorise perfusion changes as normal, delayed, reduced, reduced and

delayed as well as perfusion loss [22]. Using dedicated post-processing tools, these data can be displayed in 3D [23], (Fig. 1c, d, e).

In addition to quantitative and qualitative scoring methods, clinical practice relies on visual assessment. It should be feasible to introduce an MR scoring system that is comparable to CT [24–26]. Up to now published studies either used a modified Brody [15] or an adapted Bhalla/Helbich score [14]. None of theses scores was tested for reproducibility. Besides morphology, functional parameters are important for a comprehensive diagnosis and have to be integrated into a dedicated MR score, also to generate an additional benefit over CT. A recently presented morpho-functional MRI score is easily applicable and reproducible for the semi-quantitative morphological and functional evaluation of a large severity spectrum of CF lung disease [27].

Based on the current state of affairs, perfusion MRI can be applied to monitor therapy and may be capable of differentiating between regions with reversible and irreversible disease. In contrast to CT [24–26, 28, 29] a dedicated scoring system as well as quantitative readouts for pulmonary MRI is lacking and will require development.

Acute pulmonary embolism in young or pregnant patients

The current imaging reference technique in evaluation of acute pulmonary embolism is helical computed tomography [30]. Its major advantage over ventilation and perfusion scintigraphy

and SPECT are the availability and the comparably short acquisition time of the study with almost immediate delivery of the necessary information for patient care [30]. However, radiation exposure by CT is significant; therefore an alternative method for young patients and pregnant women would be appreciated. To be competitive with CT, an abbreviated MR protocol focusing on lung vessel imaging and lung perfusion may be accomplished within 15 min in-room time.

Although MR angiography has been demonstrated as an excellent tool in dedicated centres [31], more recent data from a large multicentre study suggest that the technique in isolation produced unsatisfactory results [32]. Therefore, combinations of different available MRI techniques for the detection of pulmonary embolism may be of better value [33]. This protocol was further modified and extended into a two-step algorithm [9]. As a first step, a steady-state GRE sequence acquired in two or three planes during free breathing would serve for an early detection of large central emboli within the first 5 min of the examination—according to the literature with a sensitivity of 90% and a specificity of close to 100% [33–35]. Any patient with a massive, central embolism detected at this point could be directly referred to intensive care and treatment; the time to diagnosis would be at least as short as with contrast-enhanced helical CT. If this first step of the examination produces a negative or unclear result, the protocol would be continued with the contrast-enhanced steps including first pass perfusion imaging, high spatial resolution contrast-enhanced (CE) MRA

Fig. 2 A 55-year-old patient with acute pulmonary embolism. Coronal steady-state free precession images acquired during free breathing (a) and contrast-enhanced coronal 3d flash angiogram acquired in breathhold (b; embolus inside the right lower lobe artery circled); c series of subtracted images from the first pass perfusion study, perfusion deficits marked with open arrows at the image obtained at peak lung enhancement; 1.5-T MRI scanner
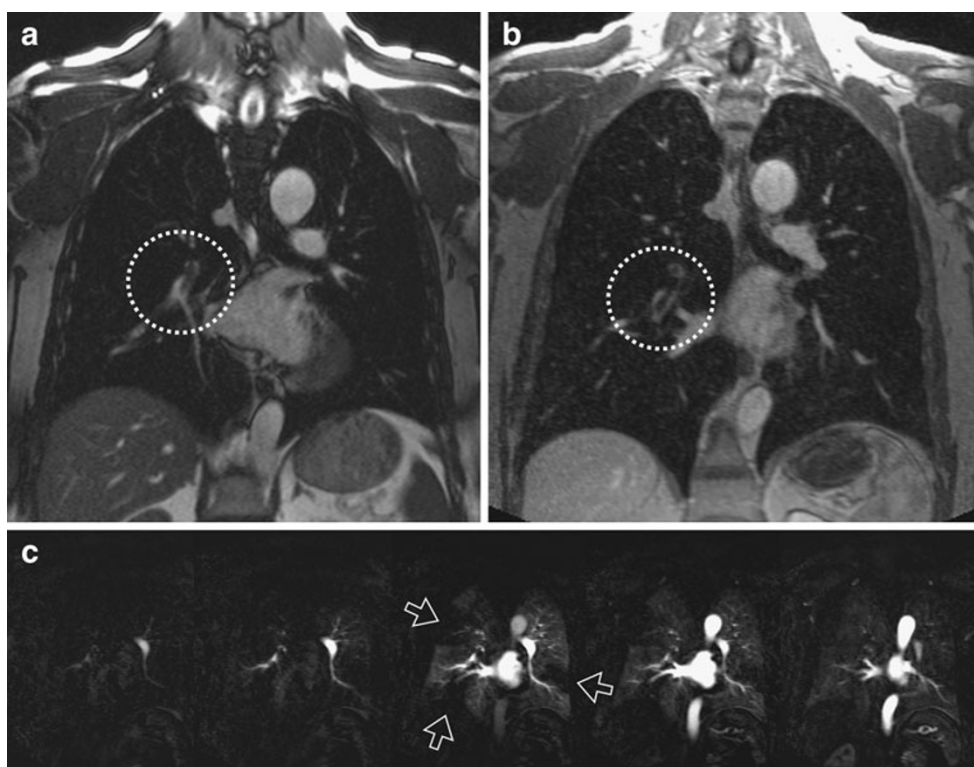
and a final acquisition with a volumetric interpolated 3D FLASH sequence in transverse orientation (Fig. 2). Despite its composition of multiple sequences, the two-step examination could be completed within 15 min in-room time, which makes it feasible as a quick test for daily clinical routine. In many cases, such as in pregnant woman, when administration of contrast material or radiation exposure is contra-indicated, the examination can be limited to the first step, the free breathing or breathhold acquisition of steady-state GRE sequences alone. Furthermore, since these steps are partially redundant, at least one acquisition would be expected to be diagnostic even in non-compliant patients.

Lung MRI as an alternative or adjunct to other modalities

Central mass with atelectasis and pleural effusion

Undoubtedly, contrast-enhanced multiple detector row computed tomography is the method of first choice in imaging thoracic malignancies. MRI is considered as an alternative method, e.g. when the application of iodinated contrast media is contraindicated. For this purpose, MRI with dedicated standard protocols can provide a comprehensive morphologic TNM evaluation [36]. A contrast-enhanced examination can be achieved within 25 min in-room time. Intra-pulmonary masses larger than the clinically relevant size of 4–5 mm in diameter can be easily detected. The extent of mediastinal, hilar and supraclavicular lymph node enlargment can be assessed with excellent soft tissue contrast. Metastatic disease involving the liver, the adrenal glands and the skeleton of the thorax are fully covered. The feasibility of extending the examination to whole-body staging with comparable results as achieved by PET/CT has been demonstrated [37–40]. The only limitation compared to CT is the detection of nodules smaller than the clinically relevant size of 4–5 mm. Beyond being just a surrogate for a CT scan in some cases, MRI can offer additional advantages. In large pulmonary masses, the excellent soft tissue contrast of MRI allows for the distinction of tumour from atelectasis and pleural effusion, e.g. for image-guided radiotherapy planning. Administration of T1-shortening contrast material specifically contributes to detecting tumour necrosis, chest wall or mediastinal invasion, and pleural reaction/carcinomatosis [8] (Fig. 3). Furthermore, MRI contributes comprehensive functional information on respiratory mechanics, tumour mobility [41] and lung perfusion [42, 43]. The clinical value of complementing the purely morphologic staging by imaging of perfusion and tumour motion in specific clinical settings and situations has been demonstrated and is subject to further investigation.
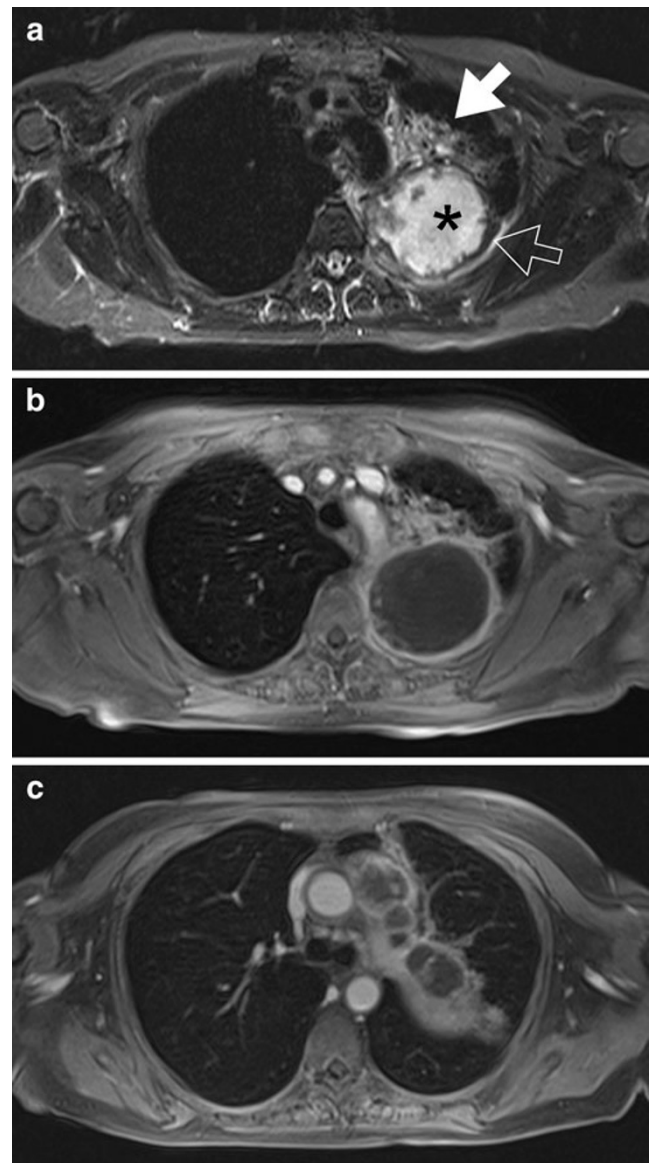

Fig. 3 A 56-year-old female patient with small cell lung cancer. The transverse T2-weighted fat-saturated (**a**) and T1-weighted contrast-enhanced fat-saturated 3D-GRE images (**b**, **c**) show a large, centrally necrotic mass in the left upper lobe with large peri-hilar lymph node metastases. Note the high soft tissue contrast between alelectatic lung (open arrow), small rim of solid tumour (filled arrow) and colliquated central portion of the mass (asterisk)

Pneumonia in young patients

The potential of MRI to replace chest radiography, particularly in very young children, was already investigated several years ago [18, 44–46]. Much of this work was conducted on low-field MRI (mainly 0.2-T scanners) using steady-state free precession sequences [47]. On average, three thick slices are acquired in coronal orientation with a mean breathhold time of 4–5 s. However, nowadays, only a few institutions regularly use low-field lung MRI in paediatric

radiology. Nevertheless, the experience from this work may be considered valid for the suggested protocols for 1.5-T scanners since image quality has significantly improved. Therefore, T2-weighted fat-suppressed as well as dynamic contrast-enhanced T1-GRE sequences are applied with a slice thickness between 5 and 6 mm [48]. Disease entities encompassing community-acquired pneumonia, empyema, fungal infections and chronic bronchitis are detectable [49] (Fig. 4).
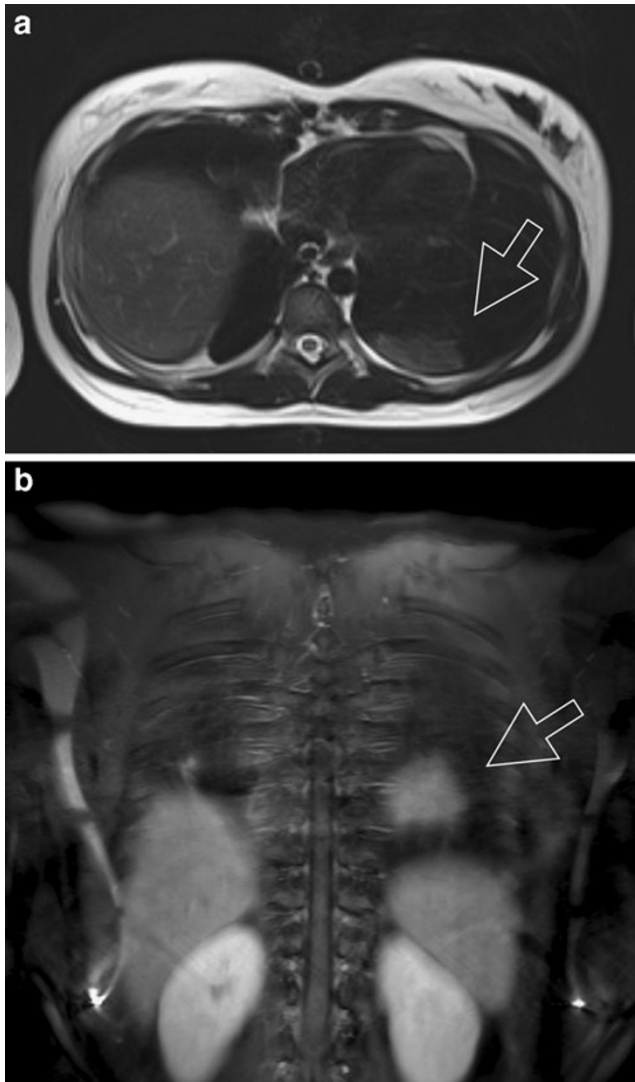

Fig. 4 A 13-year-old girl with suspected organising pneumonia (BOOP) in both lungs. Transverse T2-weighted TSE images (**a**) were acquired with the navigator technique (sample volume placed on the dome of the right liver lobe). The *open arrow* indicates an oval-shaped consolidation with pleural contact in the lower left lobe and moderate signal intensity. Coronal contrast-enhanced fat-saturated T1-weighted GRE images (**b**) were acquired with the breathhold technique. The *open arrow* indicates the oval-shaped consolidation in the lower left lobe with contrast enhancement; this is interpreted as an indicator of an active inflammatory process

Recent studies demonstrated the feasibility of chest examinations on 3-T high-field MRI. ECG triggering seems to be mandatory to reduce pulsation artefacts. One study used the navigator techniques to reduce breathing artefacts. High-field chest MRI may allow differentiation between inflammation- and fibrosis-predominant lesions in UIP and NSIP in adult patients [50]. Moreover, a recent comparison between 3-T lung MRI and HRCT as gold standard showed an excellent correlation with non-cystic fibrosis chronic lung disease in children [51]. Breathhold T2- as well as T1-weighted sequences with ECG triggering were acquired. In summary, lung MRI may prove to become a valuable tool for detection as well as characterisation of inflammatory lung disease in children.

Clinical scenarios in which CT remains the first choice modality

Emphysema/COPD

Chronic obstructive pulmonary disease (COPD) is one of the leading causes of morbidity and mortality worldwide. At present it is the fourth most common cause of death among adults, but its prevalence is increasing [52]. COPD is characterised by incompletely reversible airflow obstruction due to a mixture of airway obstruction (obstructive bronchiolitis) and parenchymal destruction (emphysema) [52]. Severity of COPD is clinically assessed by lung function tests and diffusion capacity for carbon monoxide. CT is considered the reference standard for imaging COPD-related morphological changes. Imaging COPD with proton MRI is a major challenge due to the loss of lung tissue and reduced blood volume due to hypoxic vasoconstriction combined with hyperinflation, all resulting in a marked reduction of lung parenchymal signal [53]. The strength of MRI for imaging COPD lies with the assessment of functional parameters like perfusion and respiratory dynamics [54].

In COPD emphysematous destruction is difficult to diagnose because of a loss of MR signal. Hyperinflation severely affects diaphragmatic geometry with subsequent reduction of the mechanical properties, while the accessory neck and rib muscles become less effective [55]. The common clinical measurements of COPD do not provide insights into how structural alterations in the lung lead to dysfunction in the breathing mechanics, although treatments such as lung volume reduction surgery (LVRS) are thought to improve lung function by facilitating breathing mechanics and increasing elastic recoil [56].

In contrast to normal subjects with regular, synchronous diaphragm and chest wall motion, patients with emphysema frequently have reduced, irregular or asynchronous motion, with a significant decrease in the maximum amplitude and

the length of apposition of the diaphragm [57]. In some patients the diaphragm movement is not coordinated (e.g. the ventral portion of the hemidiaphragm moves inferiorly while the dorsal part moves cranially [58]), while paradoxical diaphragmatic motion correlated with mild and moderate hyperinflation [59].

One study demonstrated a correlation between the change of parenchymal signal intensity measured by MRI at inspiration and expiration and FEV_1 (r=0.508) as a predictor of airflow obstruction [60].

Several studies have shown that airway obstruction in patients with COPD tends to be located in airways smaller than 2 mm internal diameter [61]. These airways are located between the 4th and the 14th generation of the tracheobronchial tree. Severe peripheral airflow obstruction also affects the proximal airways from subsegmental bronchi to trachea. For the assessment of tracheal instability, such as seen in tracheobronchial malacia (which may mimic the clinical appearance of small airways disease), MR cine acquisitions during continuous respiration or forced expiration can be recommended [62]. The depiction of airway dimensions and size of the airway walls by MRI in physiological condition is limited to the central bronchial tree. For the depiction of bronchiectasis, sequences with a high spatial resolution are essential (see section on CF). The previously described 3D volume interpolated gradient echo sequence (VIBE) offers a sufficient spatial resolution with a sensitivity of 79% and a specificity of 98% regarding visual depiction of bronchiectasis compared to CT [3].

Gas exchange in the lungs is optimally maintained by matching of ventilation and perfusion. In patients with COPD, ventilation is impaired due to airway obstruction and parenchymal destruction. In regions with reduced ventilation, hypoxic vasoconstriction occurs [63, 64] causing a reduction of local pulmonary blood flow with redistribution to better ventilated lung regions [65, 66]. The reduction of the pulmonary vascular bed is related to the severity of parenchymal destruction; however the distribution of perfusion does not necessarily match parenchymal destruction [67, 68]. Conventional radionuclide perfusion scintigraphy has been used to assess these abnormalities, but it has substantial limitations with respect to spatial and temporal resolution.

MR perfusion allows for a high diagnostic accuracy in detecting perfusion abnormalities of the lung [69, 70]. Additionally, MR perfusion ratios correlate well with radionuclide perfusion scintigraphy ratios [71, 72]. Lobar and segmental analysis of the perfusion defects can be performed [68]. Perfusion abnormalities in COPD clearly differ from those caused by vascular obstruction. While wedge-shaped perfusion defects occur in embolic obstruction, a generally low degree of inhomogeneous contrast enhancement is found in COPD with emphysema [73]. Furthermore,

the peak signal intensity is reduced. These features allow for easy visual differentiation and compare well with work done using CT perfusion experiments [74]. In patients with COPD the quantitative evaluation of 3D perfusion showed that the mean pulmonary blood flow (PBF), pulmonary blood volume (PBV) and mean transit time (MTT) are diffusely decreased and the changes are heterogeneous [75]. Calculated mean PBF and PBV are significantly decreased, and MTT is significantly shortened [76].

Interstitial lung disease

Interstitial lung disease (ILD) encompasses numerous pathologic disorders of different etiologies, generally manifesting with an inflammatory reaction known as "alveolitis", which may progress towards fibrosis. Because the nature of these disorders is highly heterogeneous, imaging findings alone are often insufficient for making the final diagnosis, and integration of morphologic aspects with clinical and functional data is required. In the last 3 decades, computed tomography (CT) has clarified the elementary alterations and morphologic patterns characterising the infiltrative changes of ILD. In contrast, MRI has only recently overcome many of the technical issues related to lung imaging, providing a standardised image quality, which in many instances is now comparable to CT. This partly explains the relatively limited number of MRI studies that have been clinically performed in ILD patients. Nonetheless, published data suggest at least three possible applications for lung MRI in ILD: (1) visualisation and recognition of morphological changes and their patterns, (2) assessment of the inflammatory activity of the disease and (3) effects of lung morphologic changes on functional parameters such as contrast enhancement and perfusion.

The essential morphologic findings in ILD include air-space disease, interstitial abnormalities or a combination of the two. Because MR signal increases proportionally to proton density, air-space infiltrates appear on the T2-weighted images as hyperintense areas against the dark background of the normal lung parenchyma. When pulmonary vascular markings are not obscured, these areas can be assimilated to the ground-glass opacities detected by CT [17, 77]. More dense opacities appear as consolidations, which can be easily assessed by MRI [78]. Similar to consolidations, interstitial abnormalities increase signal intensity presenting with curvilinear bands, nodules and reticulations, which can be associated to a variable degree of parenchymal distortion [50, 79, 80]. Fibrotic changes that extensively involve both peripheral and perihilar portions of the lung are generally well demonstrated on T2-weighted images, albeit that one needs to consider extracellular interstitial water as a potential differential diagnosis in patients with suspected congestive heart failure. Subtle changes in the subpleural regions may become more difficult to visualise, notably when

parenchymal distortion is not present, demonstrating the superiority of CT in this respect. T1-weighted VIBE images offer higher spatial resolution, and post-contrast acquisition with fat-suppression is recommended to increase the signal of altered subpleural lung tissue against a background represented by chest wall muscles, ribs and normal lung parenchyma. Honeycombing, which manifests with reticular changes and irregular cystic transformation of the lung, can also be assessed using this technique [50] (Figs. 5, 6, 7 and 8).

Differentiation of active inflammation from fibrosis is of significant clinical importance both for the prediction of therapy response and clinical outcome of ILD. Both MR signal and contrast-enhancement characteristics of inflammation and fibrosis have been investigated. Although initial studies performed on 1.5 T lacked sufficient image quality [81–83], the feasibility of the assessment of disease activity in ILD was demonstrated. Only recently, 3.0-T MRI has increased sensitivity to changes in proton density. In particular, Yi et al. [50] reported that MR signal of inflammatory and fibrotic lesions on T2-weighted images is hyperintense and isointense, respectively, compared to the signal from chest wall muscle, indicating an increased water content in the areas of inflammation.

Dynamic MRI using iv contrast administration also indicated that early enhancement and washout with discernible peak enhancement at 1 or 3 min after contrast injection was associated with positive and negative prediction values of 82 and 92%, respectively, in predicting disease activity [50]. The earlier enhancement and rapid washout would be in agreement with higher permeability of capillaries in the areas of inflammation compared to those of fibrosis.

A different approach to differentiating active inflammation from fibrosis was attempted in a recent study in a bleomycin-induced lung injury model in rats [84]. Proton density and T2 relaxation were computed regionally in the injured lungs, and MR-derived parameters were compared to postmortem measures of water and collagen content. The authors concluded that proton density and T2 relaxation data acquired using MRI were sensitive to inflammation and fibrotic changes in the lung. Although they were able to distinguish diseased lungs as effectively as postmortem measurements, they were unable to differentiate between fibrosis and inflammation. In conclusion, these data are encouraging and support potential future applications of MRI in interstitial lung disease both in research and clinical settings.

Future perspectives

Significant efforts have been made to further improve robustness and reproducibility of lung MR image quality. Compared with x-ray and CT, the quality of lung MRI is more dependent on the ability of patients to follow breath hold instructions. Advanced acquisition schemes with inherent correction of respiratory motion and cardiac pulsation are therefore important for future developments. For example, a conjoint research group of medical physics and radiology departments supported by the German Research Foundation (Deutsche Forschungsgemeinschaft) is currently working on the development of self-navigated sequence designs and radial k-space methods for the assessment of lung morphology on free breathing. Similarly, a group of

Fig. 5 Infiltrative disorder of the lung. Typical fibrotic changes in a patient with interstitial pulmonary fibrosis. Extensive reticulation and architectural distortion predominant in the subpleural regions of the lung are well demonstrated by the axial (a, b) and coronal (c–e) MR images obtained using the half-Fourier single-shot fast spin echo (a, c, e) and post-constrast volume interpolated T1-weighted GRE (b, e) sequences
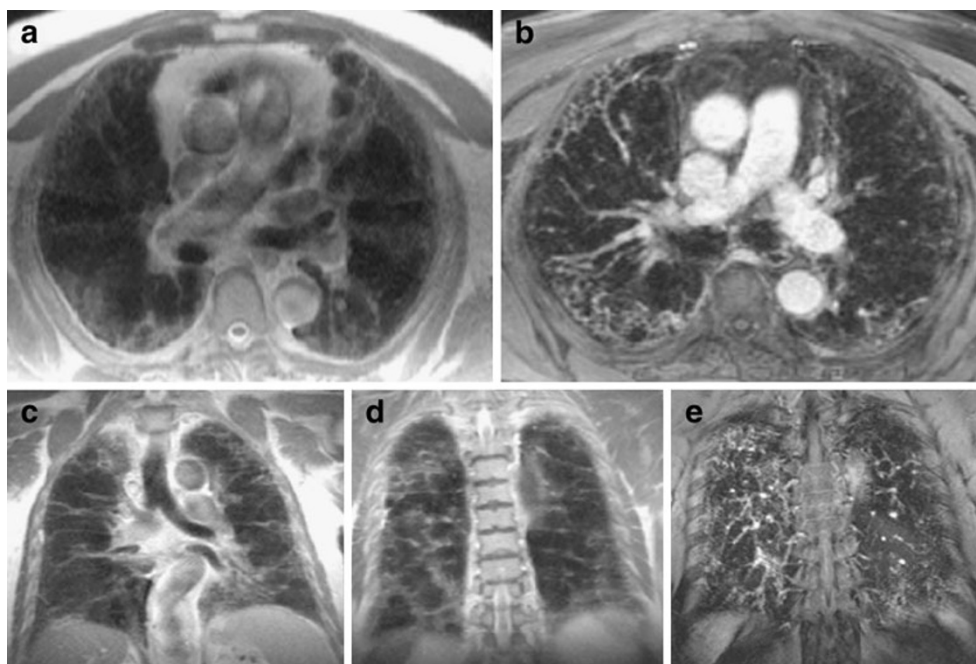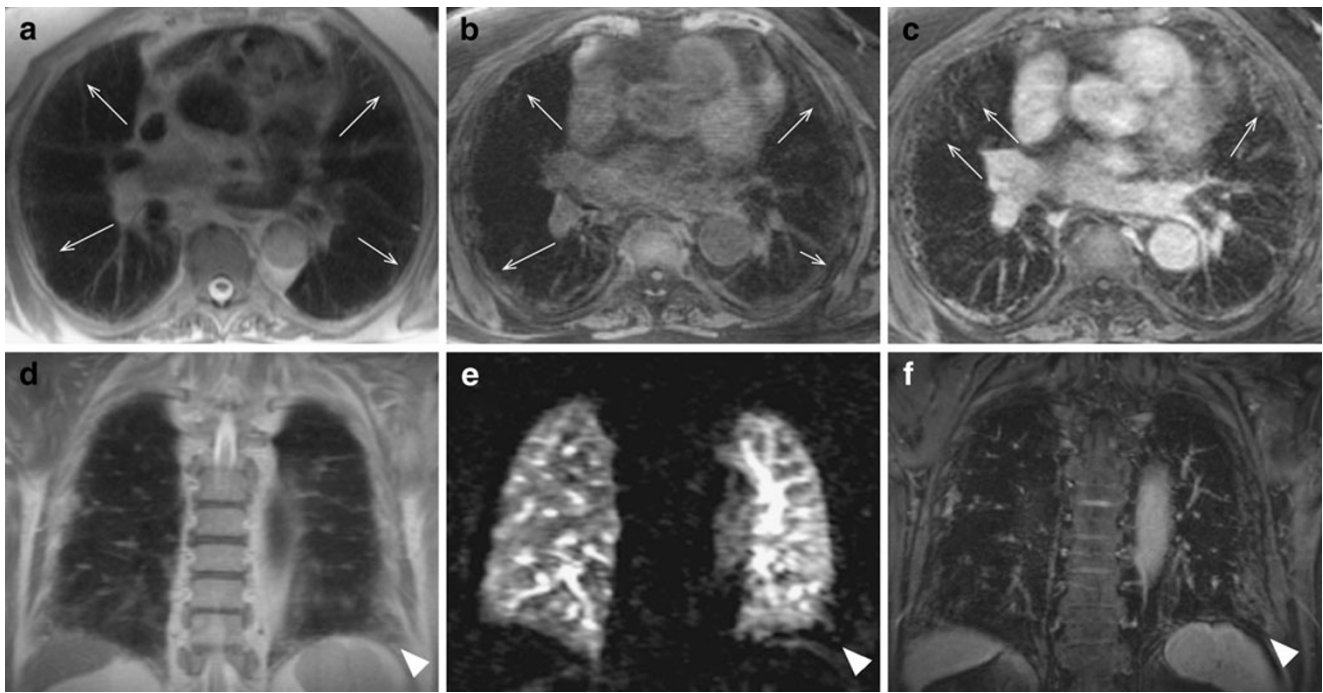
Fig. 6 Subtle subpleural reticulation in a patient with fibrotic-predominant NSIP. The interlobular reticulation (*thin arrows*) is more evident after contrast administration (**c** and **f**). A perfusion defect (*arrowhead* in **e**) is associated to the peripheral fibrotic changes at the left lateral costo-phrenic angle (*arrowheads* in **d** and **f**)

scientists in the USA is working on dedicated MR imaging in COPD within the Multi Ethnic Study of Atherosclerosis consortium with particular focus on perfusion and dynamic assessment.

One way to improve the robustness of lung MRI against respiratory motion is to implement self-navigation. The prototype 3D-MRI sequence (a self-navigated T1-weighted 3D flash with quasi-random k-space ordering) acquires multiple full lung volumes during free breathing, which results in a set of images with unsharp delineation of structures that are subject to respiratory motion. With each acquisition non-spatially encoded DC signals are acquired at the center of k-space to be used as navigator. This signal contains sufficient information to detect motion and to select image information of the different acquisitions to either produce one motion corrected data set for morphologic imaging without patient compliance or to perform a detailed motion analysis [85]. Another approach is based on radial imaging with k-space weighted image contrast (KWIC). Again, redundant data are acquired over multiple respiratory cycles. Motion correction is achieved by radial data acquisition with extraction of the signal from k-space centre for the determination of the respiratory cycle. The views are then grouped and images are reconstructed for each respiratory phase. Further improvements of image quality are achieved with autofocusing, 3D image correlation, K-space-weighted image contrast (KWIC) and principal component analysis [86–88].

Fig. 7 Fibrosis associated with rounded consolidation. **a**) Subpleural reticular changes are visualised at the periphery of the lungs (*thin arrows*). **b**) After contrast administration the subtle linear enhancement at the pulmonary-chest wall interface indicates abnormal findings related to subpleural fibrosis (*thin arrows*). A rounded consolidation is present on the left in the lingula suspected for lung tumour in ILD (*asterisk*)
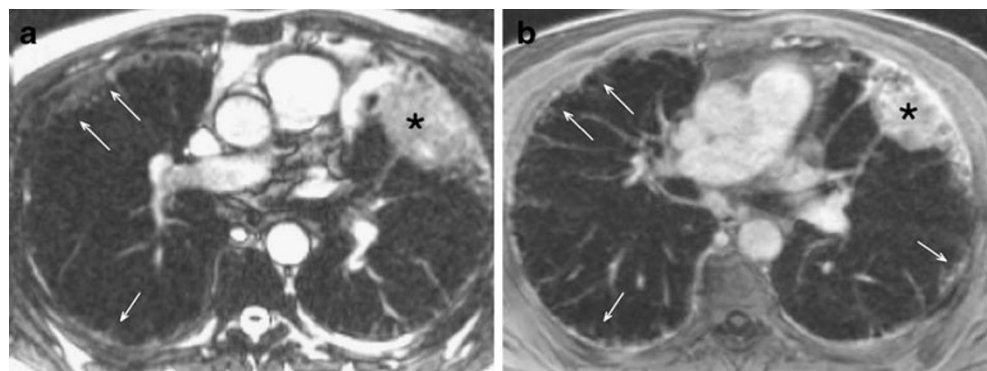
Fig. 8 Bilateral hilar and mediastinal adenomegalies in sarcoidosis. Node enlargement (*arrows*) is demonstrated with gradient echo images before (**a**) and after administration of contrast material (**b**). Coronal perfusion images indicate vascular compression at the right hilum (*arrow*, **c**) and a wedge-shaped perfusion defect (*asterisk*, **d**)
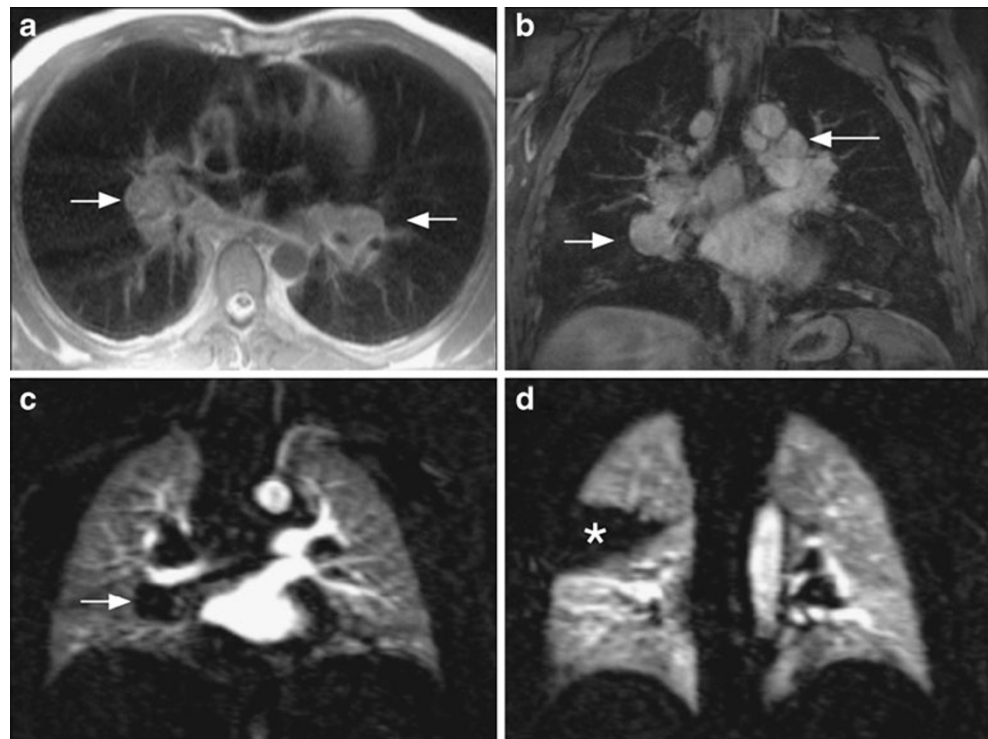

Fig. 9 Twenty-three year-old female with acute pulmonary embolism at the time point of diagnosis (**a**, **b**) and at follow-up study after 6 months (**c**, **d**). The initial dynamic contrast enhanced (DCE) study (**a**) as well as the perfusion-weighted Fourier-decomposition (FD) image (**b**) demonstrate multiple perfusion defects (*open arrows*). In the follow up study, both techniques (DCE; **c** and FD; **d**) demonstrate an almost homogeneous lung perfusion after effective anticoagulation
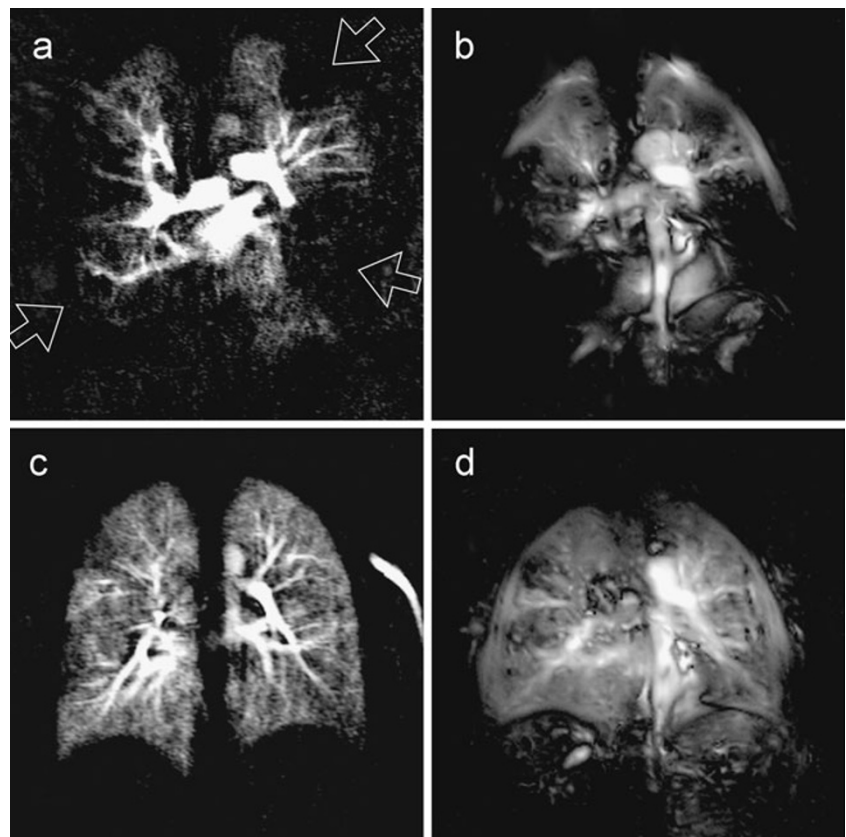
Non-contrast-enhanced ventilation-perfusion scanning—poor man's "have it all"?

One of the latest developments in the field of proton-based lung MRI appears to be a very promising technology for non-contrast-enhanced ventilation and perfusion scanning. This novel approach, known as Fourier decomposition MRI [89], utilises a short echo dynamic SSFP acquisition of lung images with subsequent compensation for respiratory motion by using nonrigid image registration [90]. Spectral analysis of the image time series allows for identification of peaks at the respiratory and cardiac frequencies. Amplitude of these peaks is related to regional proton density change caused by deformation of lung parenchyma (highest signal with lowest pulmonary air content in expiration) and pulmonary blood flow (lowest signal with maximum blood flow in systole) [91]. Further image post-processing produces ventilation- and perfusion-weighted maps for regional assessment of lung function from a single acquisition series. However, the quantitative validation remains subject to further investigation (Fig. 9) [92]. Nevertheless, there is a perspective that the method of choice for morphologic and functional assessment of acute pulmonary embolism in the very near future might be a non-contrast-enhanced free breathing MR scan of 10–15 min.

Hybrid PET/MRI

Hybrid PET/MRI has recently become available for clinical research. Compared to PET/CT, PET/MRI may be advantageous due to higher soft tissue contrast, while there is a slight reduction in ionising radiation dose [93]. Technically, integration of the two systems has been a significant challenge and required substantial modifications [94–96]. The size of the PET detectors had to be minimised; a PET detector that is insensitive to high magnetic fields had to be developed, and the adverse effect of PET detector parts on the homogeneity of the magnet's B0 field must be minimised. Moreover, interference between the radiofrequency signals, MRI gradients and PET electronic signals must be avoided [97]. Some of these problems were overcome by application of optical fibres and advances in gamma ray detector technology, which were initiated mainly by the advent of avalanche photodiodes; in addition the routine availability of fast scintillation materials resulted in the development of fully magnetic-field-insensitive high-performance PET detectors [98]. More recently, a truly integrated 3-T MRI/PET system was launched.

Although PET/MRI may not necessarily replace the role of PET/CT in thoracic oncological imaging [99], and specific clinical indications remain to be identified, MRI may be advantageous when compared to CT in the investigation of consolidating lung lesions, and malignant mediastinal and chest wall invasion. The additional diagnostic value of PET/MRI over PET/CT on nodal staging is questionable since both MRI and CT nodal staging is size based [100]. MRI, however, has been reported to be of higher accuracy than PET/CT when assessing the brain, liver and the bone for distant metastases [101]. Oncological research may be another potential area where multiple follow-up functional and anatomical imaging by PET/MRI may be advantageous over PET/CT. Lastly, with the increasing availability of radiotracers and novel compounds for molecular and physiological assessment, including labelling of target cells and compounds that target particular cell lines or processes, the combination of these powerful modalities may result in significant advances for research (and potentially clinical) purposes.

Conclusions

MRI is emerging as a valuable lung imaging modality, together with x-ray and CT. It offers a unique combination of morphological and functional information in a single examination without any radiation burden to the patient. However, although "push-button" protocols facilitate its clinical application, lung MRI can be still challenging, being the most comprehensive but also most expensive and least robust of the three modalities. New users are advised to make themselves familiar with the particular advantages and limitations of the technique and its diagnostic scope to appreciate its potential benefits. Given this, lung MRI will be increasingly used and even further improved by additional recent and future developments, in particular in the fields of motion compensation and functional imaging.

References

1. Puderbach M, Hintze C, Ley S, Eichinger M, Kauczor H-U, Biederer J (2007) MR imaging of the chest: a practical approach at 1.5T. Eur J Radiol 64:345–355
2. Biederer J, Hintze C, Fabel M, Jakob PM, Horger W, Graessner J, Bolster BD, Heller M (2011) MRI of the lung—ready…get set… go! Magnetom Flash 46:6–15
3. Biederer J, Both M, Graessner J, Liess C, Jakob P, Reuter M, Heller M (2003) Lung morphology: fast MR imaging assessment with a volumetric interpolated breath-hold technique: initial experience with patients. Radiology 226:242–249
4. Biederer J, Reuter M, Both M, Muhle C, Grimm J, Graessner J, Heller M (2002) Analysis of artefacts and detail resolution of lung MRI with breath-hold T1-weighted gradient-echo and T2-weighted fast spin-echo sequences with respiratory triggering. Eur Radiol 12:378–384
5. Biederer J, Hintze C, Fabel M (2008) MRI of pulmonary nodules: technique and diagnostic value. Cancer Imaging 8:125–130

6. Biederer J, Schoene A, Freitag S, Reuter M, Heller M (2003) Simulated pulmonary nodules implanted in a dedicated porcine chest phantom: sensitivity of MR imaging for detection. Radiology 227:475–483

7. Biederer J, Busse I, Grimm J, Reuter M, Muhle C, Freitag S, Heller M (2002) Sensitivity of MRI in detecting alveolar Infiltrates: experimental studies. Rofo 174:1033–1039

8. Hintze C, Dinkel J, Biederer J, Heussel CP, Puderbach M (2010) New procedures. Comprehensive staging of lung cancer by MRI. Radiologe 50:699–705

9. Biederer J, Bauman G, Hintze C, Fabel M, Both M (2011) Magnetresonanztomographie. Der Pneumologe 8:234–242

10. Stern M, Wiedemann B, Wenzlaff P (2008) From registry to quality management: the German Cystic Fibrosis Quality Assessment project 1995 2006. Eur Respir J 31:29–35

11. Gibson RL, Burns JL, Ramsey BW (2003) Pathophysiology and management of pulmonary infections in cystic fibrosis. Am J Respir Crit Care Med 168:918–951

12. de Jong PA, Mayo JR, Golmohammadi K, Nakano Y, Lequin MH, Tiddens HAWM, Aldrich J, Coxson HO, Sin DD (2006) Estimation of cancer mortality associated with repetitive computed tomography scanning. Am J Respir Crit Care Med 173:199–203

13. Puderbach M, Eichinger M, Gahr J, Ley S, Tuengerthal S, Schmähl A, Fink C, Plathow C, Wiebel M, Müller FM, Kauczor HU (2007) Proton MRI appearance of cystic fibrosis: comparison to CT. Eur Radiol 17:716–724

14. Puderbach M, Eichinger M, Haeselbarth J, Ley S, Kopp-Schneider A, Tuengerthal S, Schmaehl A, Fink C, Plathow C, Müller FM, Kauczor HU (2007) Assessment of morphological MRI for pulmonary changes in cystic fibrosis (CF) patients: comparison to thin-section CT and chest x-ray. Invest Radiol 42:715–725

15. Failo R, Wielopolski PA, Tiddens HAWM, Hop WCJ, Mucelli RP, Lequin MH (2009) Lung morphology assessment using MRI: a robust ultra-short TR/TE 2D steady state free precession sequence used in cystic fibrosis patients. Magn Reson Med 61:299–306

16. Eichinger M, Puderbach M, Fink C, Gahr J, Ley S, Plathow C, Tuengerthal S, Zuna I, Müller F-M, Müller FM, Kauczor HU (2006) Contrast-enhanced 3D MRI of lung perfusion in children with cystic fibrosis–initial results. Eur Radiol 16:2147–2152

17. Eibel R, Herzog P, Dietrich O, Rieger CT, Ostermann H, Reiser MF, Schoenberg SO (2006) Pulmonary abnormalities in immunocompromised patients: comparative detection with parallel acquisition MR imaging and thin-section helical CT. Radiology 241:880–891

18. Rupprecht T, Böwing B, Kuth R, Deimling M, Rascher W, Wagner M (2002) Steady-state free precession projection MRI as a potential alternative to the conventional chest X-ray in pediatric patients with suspected pneumonia. Eur Radiol 12:2752–2756

19. Hatabu H, Gaa J, Kim D, Li W, Prasad PV, Edelman RR (1996) Pulmonary perfusion: qualitative assessment with dynamic contrast-enhanced MRI using ultra-short TE and inversion recovery turbo FLASH. Magn Reson Med 36:503–508

20. Theilmann RJ, Arai TJ, Samiee A, Dubowitz DJ, Hopkins SR, Buxton RB, Prisk GK (2009) Quantitative MRI measurement of lung density must account for the change in T(2) (*) with lung inflation. J Magn Reson Imaging 30:527–534

21. Puderbach M, Risse F, Biederer J, Ley-Zaporozhan J, Ley S, Szabo G, Semmler W, Kauczor H-U (2008) In vivo Gd-DTPA concentration for MR lung perfusion measurements: assessment with computed tomography in a porcine model. Eur Radiol 18:2102–2107

22. Risse F, Eichinger M, Kauczor H-U, Semmler W, Puderbach M (2011) Improved visualization of delayed perfusion in lung MRI. Eur J Radiol 77:105–110

23. Kuder TA, Risse F, Eichinger M, Ley S, Puderbach M, Kauczor H-U, Fink C (2008) New method for 3D parametric visualization of contrast-enhanced pulmonary perfusion MRI data. Eur Radiol 18:291–297

24. Bhalla M, Turcios N, Aponte V, Jenkins M, Leitman BS, McCauley DI, Naidich DP (1991) Cystic fibrosis: scoring system with thin-section CT. Radiology 179:783–788

25. Helbich TH, Heinz-Peer G, Eichler I, Wunderbaldinger P, Götz M, Wojnarowski C, Brasch RC, Herold CJ (1999) Cystic fibrosis: CT assessment of lung involvement in children and adults. Radiology 213:537–544

26. Brody AS, Kosorok MR, Li Z, Broderick LS, Foster JL, Laxova A, Bandla H, Farrell PM (2006) Reproducibility of a scoring system for computed tomography scanning in cystic fibrosis. J Thorac Imaging 21:14–21

27. Eichinger M, Optazaite D-E, Kopp-Schneider A, Hintze C, Biederer J, Niemann A, Mall MA, Wielpütz MO, Kauczor H-U, Puderbach M (2011) Morphologic and functional scoring of cystic fibrosis lung disease using MRI. Eur J Radiol

28. de Jong PA, Tiddens HAWM (2007) Cystic fibrosis specific computed tomography scoring. Proc Am Thorac Soc 4:338–342

29. Santamaria F, Grillo G, Guidi G, Rotondo A, Raia V, de Ritis G, Sarnelli P, Caterino M, Greco L (1998) Cystic fibrosis: when should high-resolution computed tomography of the chest be obtained? Pediatrics 101:908–913

30. Stein PD, Fowler SE, Goodman LR, Gottschalk A, Hales CA, Hull RD, Leeper KV, Popovich J, Quinn DA, Sos TA, Sostman HD, Tapson VF, Wakefield TW, Weg JG, Woodard PK (2006) Multidetector computed tomography for acute pulmonary embolism. N Engl J Med 354:2317–2327

31. Oudkerk M, van Beek EJR, Wielopolski P, van Ooijen PMA, Brouwers-Kuyper EMJ, Bongaerts AHH, Berghout A (2002) Comparison of contrast-enhanced magnetic resonance angiography and conventional pulmonary angiography for the diagnosis of pulmonary embolism: a prospective study. Lancet 359:1643–1647

32. Stein PD, Gottschalk A, Sostman HD, Chenevert TL, Fowler SE, Goodman LR, Hales CA, Hull RD, Kanal E, Leeper KV Jr, Nadich DP, Sak DJ, Tapson VF, Wakefield TW, Weg JG, Woodard PK (2008) Methods of Prospective Investigation of Pulmonary Embolism Diagnosis III (PIOPED III). Semin Nucl Med 38:462–470

33. Kluge A, Luboldt W, Bachmann G (2006) Acute pulmonary embolism to the subsegmental level: diagnostic accuracy of three MRI techniques compared with 16-MDCT. AJR Am J Roentgenol 187:W7–W14

34. Kluge A, Gerriets T, Stolz E, Dill T, Mueller K-D, Mueller C, Bachmann G (2006) Pulmonary perfusion in acute pulmonary embolism: agreement of MRI and SPECT for lobar, segmental and subsegmental perfusion defects. Acta Radiol 47:933–940

35. Kluge A, Gerriets T, Müller C, Ekinci O, Neumann T, Dill T, Bachmann G (2005) Thoracic real-time MRI: experience from 2200 examinations in acute and ill-defined thoracic diseases. Rofo 177:1513–1521

36. Hintze C, Biederer J, Wenz HW, Eberhardt R, Kauczor HU (2006) MRI in staging of lung cancer. Radiologe 46(251–4):256–259

37. Yi CA, Shin KM, Lee KS, Kim B-T, Kim H, Kwon OJ, Choi JY, Chung MJ (2008) Non-small cell lung cancer staging: efficacy comparison of integrated PET/CT versus 3.0-T whole-body MR imaging. Radiology 248:632–642

38. Ohba Y, Nomori H, Mori T, Ikeda K, Shibata H, Kobayashi H, Shiraishi S, Katahira K (2009) Is diffusion-weighted magnetic resonance imaging superior to positron emission tomography with fludeoxyglucose F 18 in imaging non-small cell lung cancer? J Thorac Cardiovasc Surg 138:439–445

39. Mori T, Nomori H, Ikeda K, Kawanaka K, Shiraishi S, Katahira K, Yamashita Y (2008) Diffusion-weighted magnetic resonance

imaging for diagnosing malignant pulmonary nodules/masses: comparison with positron emission tomography. J Thorac Oncol 3:358–364

40. Qi LP, Zhang XP, Tang L, Li J, Sun YS, Zhu GY (2009) Using diffusion-weighted MR imaging for tumor detection in the collapsed lung: a preliminary study. Eur Radiol 19:333–341

41. Akata S, Kajiwara N, Park J, Yoshimura M, Kakizaki D, Abe K, Hirano T, Ohira T, Tsuboi M, Kato H (2008) Evaluation of chest wall invasion by lung cancer using respiratory dynamic MRI. J Med Imaging Radiat Oncol 52:36–39

42. Ohno Y, Koyama H, Takenaka D, Nogami M, Maniwa Y, Nishimura Y, Ohbayashi C, Sugimura K (2008) Dynamic MRI, dynamic multidetector-row computed tomography (MDCT), and coregistered 2-[fluorine-18]-fluoro-2-deoxy-D-glucose-positron emission tomography (FDG-PET)/CT: comparative study of capability for management of pulmonary nodules. J Magn Reson Imaging 27:1284–1295

43. Pauls S, Mottaghy FM, Schmidt SA, Krüger S, Möller P, Brambs H-J, Wunderlich A (2008) Evaluation of lung tumor perfusion by dynamic contrast-enhanced MRI. Magn Reson Imaging 26:1334–1341

44. Hebestreit A, Schultz G, Trusen A, Hebestreit H (2004) Follow-up of acute pulmonary complications in cystic fibrosis by magnetic resonance imaging: a pilot study. Acta Paediatr 93:414–416

45. Cohen MD, Eigen H, Scott PH, Tepper R, Cory DA, Smith JA, Scales RL (1986) Magnetic resonance imaging of inflammatory lung disorders: preliminary studies in children. Pediatr Pulmonol 2:211–217

46. Abolmaali ND, Schmitt J, Krauss S, Bretz F, Deimling M, Jacobi V, Vogl TJ (2004) MR imaging of lung parenchyma at 0.2T: evaluation of imaging techniques, comparative study with chest radiography and interobserver analysis. Eur Radiol 14:703–708

47. Wagner M, Böwing B, Kuth R, Deimling M, Rascher W, Rupprecht T (2001) Low field thoracic MRI–a fast and radiation free routine imaging modality in children. Magn Reson Imaging 19:975–983

48. Peltola V, Ruuskanen O, Svedström E (2008) Magnetic resonance imaging of lung infections in children. Pediatr Radiol 38:1225–1231

49. Hirsch W, Sorge I, Krohmer S, Weber D, Meier K, Till H (2008) MRI of the lungs in children. Eur J Radiol 68:278–288

50. Yi CA, Lee KS, Han J, Chung MP, Chung MJ, Shin KM (2008) 3-T MRI for differentiating inflammation- and fibrosis-predominant lesions of usual and nonspecific interstitial pneumonia: comparison study with pathologic correlation. AJR Am J Roentgenol 190:878–885

51. Montella S, Santamaria F, Salvatore M, Pignata C, Maglione M, Iacotucci P, Mollica C (2009) Assessment of chest high-field magnetic resonance imaging in children and young adults with noncystic fibrosis chronic lung disease: comparison to high-resolution computed tomography and correlation with pulmonary function. Invest Radiol 44:532–538

52. Mannino DM, Doherty DE, Sonia Buist A (2006) Global Initiative on Obstructive Lung Disease (GOLD) classification of lung disease and mortality: findings from the Atherosclerosis Risk in Communities (ARIC) study. Respir Med 100:115–122

53. Bankier AA, O'Donnell CR, Mai VM, Storey P, De Maertelaer V, Edelman RR, Chen Q (2004) Impact of lung volume on MR signal intensity changes of the lung parenchyma. J Magn Reson Imaging 20:961–966

54. Ley-Zaporozhan J, Ley S, Kauczor H-U (2008) Morphological and functional imaging in COPD with CT and MRI: present and future. Eur Radiol 18:510–521

55. Decramer M, Gosselink R, Troosters T, Verschueren M, Evers G (1997) Muscle weakness is related to utilization of health care resources in COPD patients. Eur Respir J 10:417–423

56. Henderson AC, Ingenito EP, Salcedo ES, Moy ML, Reilly JJ, Lutchen KR (2007) Dynamic lung mechanics in late-stage emphysema before and after lung volume reduction surgery. Respir Physiol Neurobiol 155:234–242

57. Suga K, Tsukuda T, Awaya H, Takano K, Koike S, Matsunaga N, Sugi K, Esato K (1999) Impaired respiratory mechanics in pulmonary emphysema: evaluation with dynamic breathing MRI. J Magn Reson Imaging 10:510–520

58. Iwasawa T, Yoshiike Y, Saito K, Kagei S, Gotoh T, Matsubara S (2000) Paradoxical motion of the hemidiaphragm in patients with emphysema. J Thorac Imaging 15:191–195

59. Iwasawa T, Kagei S, Gotoh T, Yoshiike Y, Matsushita K, Kurihara H, Saito K, Matsubara S (2002) Magnetic resonance analysis of abnormal diaphragmatic motion in patients with emphysema. Eur Respir J 19:225–231

60. Iwasawa T, Takahashi H, Ogura T, Asakura A, Gotoh T, Kagei S, J-ichi N, Obara M, Inoue T (2007) Correlation of lung parenchymal MR signal intensity with pulmonary function tests and quantitative computed tomography (CT) evaluation: a pilot study. J Magn Reson Imaging 26:1530–1536

61. Hogg JC, Chu F, Utokaparch S, Woods R, Elliott WM, Buzatu L, Cherniack RM, Rogers RM, Sciurba FC, Coxson HO, Pare DP (2004) The nature of small-airway obstruction in chronic obstructive pulmonary disease. N Engl J Med 350:2645–2653

62. Heussel CP, Ley S, Biedermann A, Rist A, Gast KK, Schreiber WG, Kauczor H-U (2004) Respiratory lumenal change of the pharynx and trachea in normal subjects and COPD patients: assessment by cine-MRI. Eur Radiol 14:2188–2197

63. Euler US, Liljestrand G (1946) Observations on the pulmonary arterial blood pressure in the cat. Acta Physiol Scand 12:301–320

64. Theissen IL, Meissner A (1996) Hypoxic pulmonary vasoconstriction. Anaesthesist 45:643–652

65. Morrison NJ, Abboud RT, Müller NL, Miller RR, Gibson NN, Nelems B, Evans KG (1990) Pulmonary capillary blood volume in emphysema. Am Rev Respir Dis 141:53–61

66. Cederlund K, Högberg S, Jorfeldt L, Larsen F, Norman M, Rasmussen E, Tylén U (2003) Lung perfusion scintigraphy prior to lung volume reduction surgery. Acta Radiol 44:246–251

67. Sandek K, Bratel T, Lagerstrand L, Rosell H (2002) Relationship between lung function, ventilation-perfusion inequality and extent of emphysema as assessed by high-resolution computed tomography. Respir Med 96:934–943

68. Ley-Zaporozhan J, Ley S, Eberhardt R, Weinheimer O, Fink C, Puderbach M, Eichinger M, Herth F, Kauczor H-U (2007) Assessment of the relationship between lung parenchymal destruction and impaired pulmonary perfusion on a lobar level in patients with emphysema. Eur J Radiol 63:76–83

69. Sergiacomi G, Sodani G, Fabiano S, Manenti G, Spinelli A, Konda D, Di Roma M, Schillaci O, Simonetti G (2003) MRI lung perfusion 2D dynamic breath-hold technique in patients with severe emphysema. In Vivo 17:319–324

70. Fink C, Puderbach M, Bock M, Lodemann K-P, Zuna I, Schmähl A, Delorme S, Kauczor H-U (2004) Regional lung perfusion: assessment with partially parallel three-dimensional MR imaging. Radiology 231:175–184

71. Ohno Y, Koyama H, Nogami M, Takenaka D, Matsumoto S, Yoshimura M, Kotani Y, Sugimura K (2007) Postoperative lung function in lung cancer patients: comparative analysis of predictive capability of MRI, CT, and SPECT. AJR Am J Roentgenol 189:400–408

72. Molinari F, Fink C, Risse F, Tuengerthal S, Bonomo L, Kauczor H-U (2006) Assessment of differential pulmonary blood flow using perfusion magnetic resonance imaging: comparison with radionuclide perfusion scintigraphy. Invest Radiol 41:624–630

73. Amundsen T, Torheim G, Kvistad KA, Waage A, Bjermer L, Nordlid KK, Johnsen H, Asberg A, Haraldseth O (2002) Perfusion abnormalities in pulmonary embolism studied with perfusion MRI and ventilation-perfusion scintigraphy: an intra-modality

and inter-modality agreement study. J Magn Reson Imaging 15:386–394

74. Alford SK, van Beek EJR, McLennan G, Hoffman EA (2010) Heterogeneity of pulmonary perfusion as a mechanistic image-based phenotype in emphysema susceptible smokers. Proc Natl Acad Sci USA 107:7485–7490

75. Ohno Y, Higashino T, Takenaka D, Sugimoto K, Yoshikawa T, Kawai H, Fujii M, Hatabu H, Sugimura K (2004) MR angiography with sensitivity encoding (SENSE) for suspected pulmonary embolism: comparison with MDCT and ventilation-perfusion scintigraphy. AJR Am J Roentgenol 183:91–98

76. Ohno Y, Hatabu H, Murase K, Higashino T, Kawamitsu H, Watanabe H, Takenaka D, Fujii M, Sugimura K (2004) Quantitative assessment of regional pulmonary perfusion in the entire lung using three-dimensional ultrafast dynamic contrast-enhanced magnetic resonance imaging: preliminary experience in 40 subjects. J Magn Reson Imaging 20:353–365

77. Müller NL, Mayo JR, Zwirewich CV (1992) Value of MR imaging in the evaluation of chronic infiltrative lung diseases: comparison with CT. AJR Am J Roentgenol 158:1205–1209

78. Rieger C, Herzog P, Eibel R, Fiegl M, Ostermann H (2008) Pulmonary MRI–a new approach for the evaluation of febrile neutropenic patients with malignancies. Support Care Cancer 16:599–606

79. Lutterbey G, Gieseke J, von Falkenhausen M, Morakkabati N, Schild H (2005) Lung MRI at 3.0T: a comparison of helical CT and high-field MRI in the detection of diffuse lung disease. Eur Radiol 15:324–328

80. Lutterbey G, Grohé C, Gieseke J, von Falkenhausen M, Morakkabati N, Wattjes MP, Manka R, Trog D, Schild HH (2007) Initial experience with lung-MRI at 3.0T: comparison with CT and clinical data in the evaluation of interstitial lung disease activity. Eur J Radiol 61:256–261

81. McFadden RG, Carr TJ, Wood TE (1987) Proton magnetic resonance imaging to stage activity of interstitial lung disease. Chest 92:31–39

82. Berthezène Y, Vexler V, Kuwatsuru R, Rosenau W, Mühler A, Clément O, Price DC, Brasch RC (1992) Differentiation of alveolitis and pulmonary fibrosis with a macromolecular MR imaging contrast agent. Radiology 185:97–103

83. Gaeta M, Blandino A, Scribano E, Minutoli F, Barone M, Andò F, Pandolfo I (2000) Chronic infiltrative lung diseases: value of gadolinium-enhanced MRI in the evaluation of disease activity–early report. Chest 117:1173–1178

84. Jacob RE, Amidan BG, Soelberg J, Minard KR (2010) In vivo MRI of altered proton signal intensity and T2 relaxation in a bleomycin model of pulmonary inflammation and fibrosis. J Magn Reson Imaging 31:1091–1099

85. Weick S, Oechsner M, Blaimer M, Breuer H, Köstler H, Hahn D (2009) Self-gated 3D FLASH imaging of the human lung under free breathing using DC signals. Proceedings 17th Scientific Meeting, ISMRM

86. Song HK, Dougherty L (2000) k-space weighted image contrast (KWIC) for contrast manipulation in projection reconstruction MRI. Magn Reson Med 44:825–832

87. Song HK, Dougherty L (2004) Dynamic MRI with projection reconstruction and KWIC processing for simultaneous high spatial and temporal resolution. Magn Reson Med 52:815–824

88. Lin W, Guo J, Rosen MA, Song HK (2008) Respiratory motion-compensated radial dynamic contrast-enhanced (DCE)-MRI of chest and abdominal lesions. Magn Reson Med 60:1135–1146

89. Bauman G, Puderbach M, Deimling M, Jellus V, Chefd'hotel C, Dinkel J, Hintze C, Kauczor H-U, Schad LR (2009) Non-contrast-enhanced perfusion and ventilation assessment of the human lung by means of fourier decomposition in proton MRI. Magn Reson Med 62:656–664

90. Chefd'hotel C, Hermosillo G, Faugeras O (2002) Flows of Diffeomorphisms for Multimodal Image Registration. Proceedings of the IEEE International Symposium on Biomedical Imaging (ISBI'2002), Piscataway, NJ, USA: Institute of Electrical and Electronics Engineers:753–756

91. Suga K, Ogasawara N, Okada M, Tsukuda T, Matsunaga N, Miyazaki M (2002) Lung perfusion impairments in pulmonary embolic and airway obstruction with noncontrast MR imaging. J Appl Physiol 92:2439–2451

92. Bauman G, Lützen U, Ullrich M, Gaass T, Dinkel J, Elke G, Meybohm P, Frerichs I, Hoffmann B, Borggrefe J, Knuth HC, Schupp J, Prüm H, Eichinger M, Pudebach M, Biederer J, Hintze C (2011) Pulmonary functional imaging: qualitative comparison of Fourier decomposition MR imaging with SPECT/CT in porcine lung. Radiology 260:551–559

93. Pichler BJ, Judenhofer M, Pfannenberg C (2008) Multimodal imaging approaches: PET/CT and PET/MRI. In: Handb Exp Pharmacol:109–132

94. Shao Y, Cherry SR, Farahani K, Meadors K, Siegel S, Silverman RW, Marsden PK (1997) Simultaneous PET and MR imaging. Phys Med Biol 42:1965–1970

95. Pichler BJ, Kolb A, Nägele T, Schlemmer H-P (2010) PET/MRI: paving the way for the next generation of clinical multimodality imaging applications. J Nucl Med 51:333–336

96. Zaidi H, Ojha N, Morich M, Griesmer J, Hu Z, Maniawski P, Ratib O, Izquierdo-Garcia D, Fayad ZA, Shao L (2011) Design and performance evaluation of a whole-body Ingenuity TF PET-MRI system. Phys Med Biol 56:3091–3106

97. Pichler BJ, Judenhofer MS, Wehrl HF (2008) PET/MRI hybrid imaging: devices and initial results. Eur Radiol 18:1077–1086

98. Wehrl HF, Judenhofer MS, Wiehr S, Pichler BJ (2009) Pre-clinical PET/MR: technological advances and new perspectives in biomedical research. Eur J Nucl Med Mol Imaging 36(Suppl 1):S56–S68

99. Ratib O, Beyer T (2011) Whole-body hybrid PET/MRI: ready for clinical use? Eur J Nucl Med Mol Imaging 38:992–995

100. Antoch G, Bockisch A (2009) Combined PET/MRI: a new dimension in whole-body oncology imaging? Eur J Nucl Med Mol Imaging 36(Suppl 1):S113–S120

101. Antoch G, Vogt FM, Freudenberg LS, Nazaradeh F, Goehde SC, Barkhausen J, Dahmen G, Bockisch A, Debatin JF, Ruehm SG (2003) Whole-body dual-modality PET/CT and whole-body MRI for tumor staging in oncology. JAMA 290:3199–3206